Conservation of targeting but divergence in function and quality control of peroxisomal ABC transporters

Zhang, Xuebin; De Marcos Lousa, Carine; Schutte-Lensink, Nellie; Ofman, Rob; Wanders, Ronald J.; Baldwin, Stephen A.

Published in:
Biochemical Journal

DOI:
10.1042/BJ20110249

Publication date:
2011

Document Version
Peer reviewed version

Conservation of targeting but divergence in function and quality control of peroxisomal ABC transporters: an analysis using cross-kingdom expression.

Xuebin Zhang[1], Carine De Marcos Lousa[2], Nellie Schutte-Lensink[3], Rob Ofman[3], Ronald J. Wanders[3], Stephen A. Baldwin[4], Alison Baker[2], Stephan Kemp[3] and Frederica L. Theodoulou[1,5]

1. Biological Chemistry Department, Rothamsted Research Harpenden, AL5 2JQ, UK
2. Centre for Plant Sciences, University of Leeds, LS2 9JT, UK
3. Laboratory Genetic Metabolic Diseases, Academic Medical Centre, Meibergdreef 9, 1105 AZ Amsterdam, The Netherlands
4. Institute of Membrane and Systems Biology, University of Leeds, LS2 9JT, UK
5. To whom correspondence should be addressed. Email: freddie.theodoulou@bbsrc.ac.uk

Short title: Cross-kingdom targeting and function of peroxisomal ABC transporters

SYNPOSIS

ABC subfamily D transporters are found in all eukaryotic kingdoms and are known to play essential roles in mammals and plants; however their number, organisation and physiological contexts differ. Via cross-kingdom expression experiments, we explored the conservation of targeting, protein stability and function between mammalian and plant ABCD transporters. When expressed in tobacco epidermal cells, the mammalian ABCD proteins, adrenoleukodystrophy protein (ALDP), ALD related protein (ALDR) and PMP70 targeted faithfully to peroxisomes and P70R targeted to the ER, as in the native host. The *Arabidopsis thaliana* peroxin, AtPex19_1 interacted with human peroxisomal ABC transporters both *in vivo* and *in vitro*, providing an explanation for the fidelity of targeting. The fate of X-linked adrenoleukodystrophy disease-related mutants differed between fibroblasts and plant cells. In fibroblasts, levels of ALDP in some 'protein absent' mutants were increased by low-temperature culture, in some cases restoring function. In contrast, all mutant ALDP proteins examined were stable and correctly targeted in plant cells, regardless of their fate in fibroblasts. ALDR complemented the seed germination defect of the Arabidopsis *cts-1* mutant which lacks the peroxisomal ABCD transporter, CTS, but neither ALDR nor ALDP was able to rescue the defect in fatty acid β-oxidation in establishing seedlings. Taken together, the data indicate that the mechanism for trafficking of peroxisomal membrane proteins is shared between plants and mammals, but suggest differences in the sensing and turnover of mutant ABC transporter proteins and differences in substrate specificity and/or function.

KEYWORDS: ABC transporter, Pex19, peroxisome, X-ALD, ALDP, PMP70, CTS

ABBREVIATONS: ABC, ATP binding cassette; ALDP, adrenoleukodystrophy protein; ALDR, adrenoleukodystrophy related protein; CTS, comatose; FA-CoA, fatty acyl CoA;

NBD, nucleotide binding domain; PMP, peroxisomal membrane protein; PMP70, 70 kDa peroxisomal membrane protein; P70R, PMP70-related protein; TMD, transmembrane domain; VLCFA, very long chain fatty acid; X-ALD, X-linked Adrenoleukodystrophy**.**

INTRODUCTION

Peroxisomes are near-ubiquitous organelles with a wide range of functions in different eukaryotes. The β-oxidation of fatty acids is a function shared with mitochondria in mammals but exclusive to peroxisomes in plants and yeast. The importance of these organelles is underscored by the spectrum of human diseases associated with impaired peroxisomal function [1] and also by the severe, often embryo-lethal phenotypes observed for plant mutants lacking or defective in key peroxisome proteins [2-5]. The most common human peroxisomal disorder is X-linked Adrenoleukodystrophy (X-ALD), which is characterised biochemically by the accumulation of very long chain fatty acids (VLCFA) in plasma and tissues [6,7]. The primary genetic cause of this disease is mutation of the *ABCD1* gene, which encodes an ATP Binding Cassette (ABC) transporter, Adrenoleukodystrophy protein (ALDP or ABCD1) [8]. ALDP belongs to subfamily D of the ABC protein superfamily, which has three further members in humans: Adrenoleukodystrophy-related protein (ALDR; ABCD2), 70 kDa peroxisomal membrane protein (PMP70; ABCD3) and the PMP70-related protein (P70R; ABCD4, also known as PMP69), encoded by *ABCD2-4*, respectively [9]. The human ABCD proteins are so-called "half-size" ABC transporters, containing one transmembrane domain (TMD) and one nucleotide binding domain (NBD), and thus must dimerise to form a functional transporter, which compromises 2 TMDs and 2 NBDs [10]. Although heterodimerisation between human ABCD proteins has been demonstrated *in vitro* and *in vivo*, expression patterns, protein purification, functional analysis and genetic considerations suggest that homodimerisation predominates *in vivo* and is sufficient for function (reviewed in [6,11]).

The ABCD subfamily is smaller in other organisms, with two members in baker's yeast: Pxa1p and Pxa2p. Genetic evidence indicates that these proteins form a heterodimeric transporter required for import of long chain long chain fatty-acyl CoA esters (FA-CoAs) into the peroxisome [12-14]. Increased levels of VLCFA-CoA in X-ALD fibroblasts [15] and complementation of the yeast *pxa1 pxa2Δ* mutant by human *ABCD1* [16] provided evidence that ALDP is also able to transport very long chain FA-CoA. Several lines of indirect evidence point to overlapping, but distinct substrate specificities of ALDR and ALDP. ALDR expression restores β-oxidation of C24:0 and C26:0 to *pxa1 pxa2Δ* cells, though not as efficiently as ALDP [17] and rescues β-oxidation activity and VLCFA levels in fibroblasts and *Abcd1-/-* knockout mice [6,11]. However, ALDR appears to play a specific role in the synthesis of the polyunsaturated VLCFA, docosahexaenoic acid (C22:6ω3), which requires chain-shortening of C24:6ω3 by β-oxidation [17-19]. Over-expression or pharmacological induction of PMP70 can also partially compensate for the absence of functional ALDP in X-ALD fibroblasts [20, 21] and silencing of *ABCD3* in glial cells suggests a function in C26:0 metabolism [22]. However, PMP70 has also been suggested to play a specific role in the synthesis of bile acids [23]. The biochemical function of P70R is not known but the protein has recently been shown to be localised in the ER, rather than in peroxisomes [24].

Peroxisomal ABCD proteins encoded in plant genomes are full-size transporters, which are considered to represent "fused heterodimers", exemplified by the *Arabidopsis thaliana*

transporter, Comatose (CTS; also known as AtPXA1, PED3, ACN2 and AtABCD1) [25-28]. Extensive characterisation of *cts* null mutants has demonstrated key roles for CTS in seed germination, seedling establishment, root development, fertility and dark-induced senescence [25-27, 29-33]. Several of the phenotypes of *cts* mutants reflect their inability to mobilise storage triacylglycerol (TAG) and to turn over membrane lipids by β-oxidation [26, 27, 31, 32]. CTS complements the yeast *pxa1 pxa2Δ* mutant for growth on oleate and mediates β-oxidation of a range of saturated and unsaturated FA with chain lengths from C18 to C24, when expressed in yeast cells [34]. However, the functions of CTS also include acetate metabolism [28] and roles in the β-oxidation of ring-containing molecules, including 12-oxo-phytodienoic acid, the precursor of the plant hormone, jasmonic acid [35], the auxin analogue, 2,4-dichlorophenoxybutyric acid (2,4-DB) [27] and the natural auxin, indole butyric acid (IBA) [25]. Thus, in contrast to mammals, which have several peroxisomal ABC transporters with distinct roles but overlapping specificity, plant peroxisomes contain a broad specificity transporter involved in signalling and metabolism.

Peroxisomal ABC transporters, in common with other peroxisomal membrane proteins (PMPs) utilise the receptor/chaperone Pex19 for targeting and membrane insertion [36]. Recent structural data provide a plausible mechanism for targeting signal recognition, chaperone function and docking to Pex3 at the peroxisome membrane [37, 38]. Although most studies have focused on PMPs in humans and yeast, Pex19 and Pex3 appear to be conserved between animals, plants and fungi [36]. However, Pex19 proteins are rather divergent at the amino acid sequence level, and unlike animals and fungi, many plant species contain two Pex19 forms, with apparently distinct functions, as judged by RNAi studies [5]. Therefore we were curious to determine to what extent peroxisomal targeting is functionally homologous between mammals and plants and also whether ABCD functions are shared between different major taxonomic groups.

In this study, we provide evidence that Pex19 function is largely conserved between the two kingdoms and that mammalian PMPs are correctly targeted in plant cells. We found that selected "unstable" X-ALD mutants can be rescued by low-temperature culture of fibroblasts but that a wide range of missense mutants produce detectable ALDP in peroxisomes when expressed in plants, indicating that plant and mammalian cells exhibit significant differences in the fate of mutant PMPs. Furthermore, we demonstrate that the human peroxisomal ABC transporters, ALDP and ALDR, although correctly targeted when expressed in Arabidopsis, are mostly unable to substitute for the endogenous CTS transporter.

EXPERIMENTAL

Construction of plant expression plasmids

Sequence-verified IMAGE consortium collection cDNA clones [39] for subfamily D ABC transporters were obtained from GeneService (Cambridge, UK): human ABCD1 (accession no. BC015541), mouse ABCD3 (accession no. BC054446), human ABCD4 (accession no. BC012815) or Open Biosystems (Huntsville, AL, USA): human ABCD2 (accession no. BC104901). ORFs were amplified by PCR using the primer pairs shown in Table S1 to incorporate *attB* sites and recombined into the entry vector, pDONR207, and then recombined into the plant binary destination vector, En35S-Cassette b-eYFP-Nos::pCAMBIA 1300 [40], using Gateway technology (Invitrogen, Paisley, UK), to generate ABCD-YFP fusions for expression in plants. All constructs were sequenced to establish authenticity.

For nuclear mis-localisation experiments, the AtPEX19_1 ORF was amplified without its native start codon from AtPex19_1/pET28b [41], using primer pair AtPex19SalIFor/AtPex19SacIIRev and inserted into pCR4blunt (Invitrogen), to create pcR4blunt-AtPex19. A 447 bp fragment containing a nuclear localisation signal (NLS) was amplified from histone 2B (H2B) cDNA [42], using primer pair H2BSalIFor/H2BXhoIRev and inserted into pCR4blunt (Invitrogen) to create pcR4blunt-H2B. A *Sal* I-H2B-*Xho*I fragment was excised from pcR4blunt-H2B and ligated to *Sal* I-digested pcR4blunt-AtPex19-1, to create pcR4blunt-H2B-AtPex19-1. The H2B-AtPex19-1 fragment was amplified with primer pair H2BAtPex19attB1/H2BAtPex19attB2 to add *attB* sites for Gateway cloning and recombined into pDONR207-H2B-AtPex19_1 to create an entry clone. Following recombination into a Gateway-adapted pCAMBIA1300 vector to create the binary construct pCAMBIA1300-H2B-AtPex19-1, the final construct was sequenced.

Site-directed mutagenesis was carried out using the QuikChange II kit (Stratagene, La Jolla, CA), according to manufacturers' instructions. Primer sequences are given in Table S1. Constructs were sequenced to verify the presence of the mutation and to confirm that no unwanted mutations had been introduced.

Expression and purification of GST-Pex19 fusion proteins.
A human Pex19 (HsPex19) IMAGE consortium clone, accession number BC000496 [39] was obtained from GeneService (Cambridge, UK). AtPex19_1 [41] and HsPex19 were amplified with primer pairs FT119/FT120 and FT123/124, respectively, restricted with *Bam* HI/*Not* I and cloned in the corresponding sites of pGEX-4T-3 (GE Healthcare, Ltd, UK). Expression of GST fusion proteins in *E. coli* strain BL21 (DE3) was induced by IPTG (0.1 mM) for 3 h. Cells were harvested by centrifugation at 6,000 rpm for 15 min at 4 °C, resuspended in 10 ml of PBS containing 1 mM PMSF and 10 mM benzamidine and lysed by sonication. Triton X-100 and DTT were added to the lysate to give final concentrations of 1 % (v/v) and 1 mM, respectively. Following 30 min incubation at 4 °C, the lysate was clarified at 7,000 rpm for 10 min at 4°C. Fusion proteins were subjected to affinity purification using glutathione magnetic beads (Thermo Scientific, Surrey, UK), according to the manufacturers' instructions.

***In vitro* transcription/translation and pull-down assays**
ALDR and PMP70 were amplified with primer pairs FT125/FT126 and FT127/128, respectively, restricted with *Bam* HI/*Xba* I and cloned into the corresponding sites of pcDNA3.1/neo(+) (Invitrogen). ALDP/pcDNA3.1 is described in [43]. The proteins were transcribed *in vitro* from the T7-promotor, translated and labelled with FluoroTect GreenLys tRNA using the TNT Coupled Reticulocyte Lysate System (Promega, UK) following standard protocols. Purified GST fusion proteins were bound to glutathione-Sepharose beads (Thermo Scientific) in Tris-buffered saline (TBS) for 1 h at 4 °C and washed three times in phosphate buffered saline (PBS). For the *in vitro* interaction assay, 2 mg GST or GST-PEX19 protein was bound to 300 µl bead suspension and incubated were incubated with 50 µl of *in vitro* translation reaction product in 250 µl binding buffer [100 mM NaCl, 50 mM potassium phosphate pH 7.4, 1 mM $MgCl_2$, 10 % (v/v) glycerol, 0.1 % (v/v) Tween 20, 1.5 % (w/v) BSA] for 2 h at 4°C. Samples were pelleted and washed four times in 1 ml binding buffer without BSA. Pellets were resuspended in SDS-sample buffer and boiled for 3 min before being analyzed by SDS–PAGE. The gels were scanned with a Typhoon® 8600 scanner (GE Healthcare, UK), at 532 nm excitation. To confirm equal loading, the gels were silver-stained after each pull-down experiment.

Growth and transformation of Arabidopsis and tobacco plants
Tobacco (*Nicotiana tabacum*) plants were grown and transiently transformed by Agro-infiltration as described in [40, 44]. Arabidopsis (*Arabidopsis thaliana* accession Landsberg *erecta*; L*er*) plants were transformed with ALDP-YFP/pCAMBIA 1300 and ALDR-YFP/pCAMBIA 1300 by the floral dip method [45], as were *cts-1* plants and plants heterozygous for *cts-1*. The *cts-1* mutant is described in [26].

Microscopy
Confocal imaging was performed using a Zeiss inverted LSM510 laser scanning confocal microscope with an argon laser, a blue diode laser and a helium neon laser and 40x objective. For imaging co-expression of CFP and eYFP, excitation lines were 405 nm for CFP and 514 nm for eYFP. For imaging co-expression of GFP and eYFP, excitation lines 458 nm (GFP) and 514 nm (eYFP) were used alternatively with line switching in the multitracking mode of the microscope. For imaging co-expression of DAPI and eYFP, excitation lines 405 nm and 514 nm were used. Fluorescence was detected using a 505-530-nm band-pass filter for green fluorescent protein (GFP), a 530-600 nm band pass filter for enhanced yellow fluorescent protein (eYFP), 420-480 for CFP and DAPI. The pinhole was usually set to give an optical slice between 1-2.5 μm and controls were performed to prevent bleed through of fluorescence and cross-talk. Post acquisition image processing was performed using the LSM 5 browser software (Zeiss) and Adobe Photoshop (San Jose, CA) elements.

Phenotypic characterisation of plants
Germination, establishment, hypocotyl and root growth assays were performed as described in [46], unless otherwise stated. Fatty acid methyl esters were analysed as described in [47], using heneicosanoic acid, C21:0 (Nuchek-prep, Inc., Elysian, MN, USA), as an internal standard.

Fibroblast methods
Human skin fibroblasts were obtained from X-ALD patients (aged 23-63) through the Neurology Outpatient Clinic of the Academic Medical Centre. Written informed consent was received from each patient. X-ALD diagnosis was confirmed by VLCFA and *ABCD1* mutation analysis. Control fibroblasts were from male anonymous volunteers (aged 20-50). Cells were grown in HAMF10 supplemented with 10% foetal calf serum, 25 mM HEPES, 100 U/mL penicillin, 100 U/mL streptomycin and 2 mM glutamine. Cell lines were cultured in a humidified atmosphere of 5% CO_2 at 37°C. For some experiments, fibroblasts were cultured at 30°C for the time indicated, after an overnight incubation at 37°C.

Immunoblotting
Cells were harvested by trypsinisation and homogenised by sonication in PBS containing protease inhibitors. Homogenates were diluted in sample buffer before 50 μg of total protein was loaded on a 10% SDS polyacrylamide gel. Proteins were transferred to nitrocellulose by semi-dry blotting, blocked with BSA and probed with the primary monoclonal antibody against human ALDP (ALD-1D6-As, Euromedex). IRDYE 800CW (LI-COR Biosciences) goat anti-mouse IgG was used as secondary antibody. Visualization of the signal was done with the Odyssey infrared imaging system (LI-COR Biosciences). For quantification of ALDP expression levels, a calibration curve was used on each blot. The calibration curve was made by mixing different amounts of control sample (ranging from 100 to 0%) with increasing amounts of protein from an ALDP frameshift (p.Arg113fs) sample (ranging from 0% to 100%).

Quantitative RT-PCR of *ABCD1* mRNA levels

ABCD1 mRNA expression levels were determined as described [48]. mRNA was isolated from cells growing in log-phase and *PPIB* (cyclophilin B) was used as a housekeeping gene. Primer sequences are given in Table S1.

Peroxisomal β-oxidation and analysis of VLCFA in fibroblasts

Peroxisomal β-oxidation activity in whole cells using 15 μM D_3-docosanoic acid (D_3-C22:0; CDN Isotopes, Québec, Canada) was determined following our previously developed method [49]. Total cellular fatty acids were analyzed using the electrospray ionization mass spectrometry method described previously [50].

Supplementary methods

Quantification of *ABI5* transcripts

Seeds were plated on 0.5 X MS medium, containing 1 % (w/v) sucrose and dark-chilled for 2 d at 4 ºC. After 48 h, RNA was extracted using the Qiagen RNeasy kit according to the manufacturers' instructions. First-strand cDNA synthesis was carried out using SuperScript III reverse transcriptase and oligo dT (Invitrogen), according to the manufacturers' instructions. RT-PCR was carried out using the following primer pairs: ABI5for/ABI5rev and 18SrRNAfor/18SrRNArev. Quantitative PCR was carried out using the 7900HT Fast Real-Time PCR system (ABI) containing power SYBR Green for cDNA analysis in a final reaction volume of 10 μl. An alternative housekeeping primer set (GAPDHfor/GAPDHrev) gave comparable results.

Subcellular localisation of ALDP-YFP and ALDR-YFP in Arabidopsis

Transgenic lines expressing ALDP-YFP/pCAMBIA 1300 were crossed to Arabidopsis plants stably expressing CFP-SKL [40], to confirm peroxisomal localisation by confocal imaging as described in *Experimental*. Seeds from the lines PEX10-YFP [40], L*er*/ALDR-YFP and *cts-1*/ALDR-YFP were sterilised and sown on 0.5 x MS medium, stratified for 2 d at 4 ºC and transferred to a growth chamber (20 ºC; 16 h light) for 3 d. Seedlings were removed from the plates and stained with BODIPY 8 [51] as follows: a 3 mM solution of BODIPY 8 in ethanol was diluted 1:1000 in water immediately before use and seedlings were immersed in the solution for a minimum of 15 min before viewing on an LSM510 meta confocal microscope. The remaining *cts-1*/ALDR-YFP seedlings were returned to the growth chamber for 2 d then transferred to 0.5 x MS containing 1 % (w/v) sucrose and grown for a further 5 d to allow establishment, stained with BODIPY 8 and imaged as before. Excitation lines were 488 nm for eYFP and fluorescence was detected using a 505-530-nm band-pass. Excitation of BODIPY 8 was performed with a 633 nm laser and fluorescence was detected at 650 nm.

RESULTS

Mammalian ABCD proteins are correctly targeted *in planta*

In order to test the targeting of mammalian ABCD transporters in plants, the proteins were tagged at the C-terminus with enhanced yellow fluorescent protein (eYFP) and their subcellular localisation was investigated by confocal microscopy following transfection of tobacco leaves by agroinfiltration. YFP fusions of ALDP, ALDR and PMP70 were transiently expressed in the epidermal cells of plants stably expressing the peroxisomal marker, cyan fluorescent protein (CFP)-SKL (Fig. 1A-C). Peroxisomes were observed as discrete spots in the CFP channel, in the majority of cells examined. The majority of

peroxisomes were found at the cell margins, owing to the presence of the large central vacuole, characteristic of epidermal cells. Typically, agroinfiltration does not result in all of the cells being transfected (not shown); however, in cells which expressed YFP, punctate structures were observed in the YFP channel. These coincided with the peroxisomal CFP signal, as seen in the merged images. At higher magnifications (Fig. 1A-C, lower panels), the YFP signal exhibited a ring-like appearance, characteristic of peroxisomal membrane proteins, with the matrix-located CFP-SKL inside the peroxisome structure (e.g. [40]). These images indicate that ALDP, ALDR and PMP70 are all targeted to the peroxisomal membrane in plant cells, consistent with their localisation in mammalian cells. In contrast, examination of leaf sections transfected with P70R-YFP did not reveal punctate structures but rather a reticulate YFP pattern. Therefore P70R-YFP fusions were transiently expressed in leaves of tobacco plants stably expressing the ER reporter GFP-HDEL (Fig.1D). In cells where both reporters were expressed, the GFP and YFP co-localised, suggesting that P70R-YFP is located in ER, in agreement with its localisation in mammalian cells (Kashiwayama et al., 2009).

Mammalian peroxisomal ABC transporters interact with plant Pex19 *in vitro* and *in vivo*

The targeting of ALDP, ALDR and PMP70 to peroxisomes when expressed *in planta* suggests conservation of peroxisomal membrane protein targeting machinery between the animal and plant kingdoms and is consistent with studies demonstrating that PMP targeting is conserved between yeast, trypanosomes and humans [52-54]. To investigate this further, we used two independent assays to determine whether the mammalian ABC proteins interact with the receptor/chaperone protein, Arabidopsis Pex19_1 (AtPex19_1) *in vitro* and *in vivo*. In pull-down assays, *in vitro* translated peroxisomal ABC transporters bound to glutathione-*S*-transferase (GST)-AtPex19 fusions immobilised on glutathione beads (Fig. 2). In the negative controls (GST only), a small amount of binding was observed, probably due to the hydrophobic nature of the membrane proteins, but this was modest, compared to the binding observed with GST-AtPex19_1.

Interactions with Pex19 *in vivo* were tested using a nuclear mis-localisation assay [55]. AtPex19_1 and HsPex19 were fused to the nuclear localisation signal (NLS) of Arabidopsis histone 2B, [42]. Tobacco plants stably expressing CFP-SKL were co-transfected with ABCD-YFP fusions and NLS-Pex19 and examined by confocal microscopy (Fig. 3). The transfection efficiency was much lower for two genes than for one (data not shown): in some cells, the YFP signal coincided with CFP-SKL in punctate structures, indicating peroxisomal localisation of ALDP and ALDR and suggesting that NLS-Pex19 was not expressed. In some cells, no YFP signal was observed and peroxisomes were observed as blue fluorescent punctate structures. However, in a small number of cells, punctate structures were absent from the CFP channel and the YFP signal was located in large, roughly spherical structures, of which there was one per cell. These structures stained with DAPI, indicating that they are nuclei (Fig. S1). The number of cells containing YFP-positive nuclei varied between experiments (examples with a higher level of co-transfection are shown in Fig. S1, panels I-P). Using this assay, we observed interactions between HsPex19 and ALDP (Fig. 3A-D; positive control) and NLS-AtPex19_1 and both ALDP and ALDR (Fig. 3E-L), but were not able to demonstrate AtPex19-dependent mis-localisation of PMP70, possibly because PMP70 was expressed much less efficiently in tobacco epidermis than ALDP and ALDR (data not shown). Alternatively this finding might have resulted from preferential interaction of PMP70 with endogenous tobacco Pex19. Both tobacco and Arabidopsis have two Pex19 genes; it is

possible that the different Pex19 forms exhibit different affinities towards different PMPs. This remains to be tested in future studies. The loss of punctuate structures in the CFP channel is consistent with the interaction of NLS-AtPex19_1 (and also NLS-HsPex19) with endogenous peroxins, disrupting peroxisome biogenesis by drawing Pex19-binding proteins into the nucleus. This suggests that key peroxins are being turned over in tobacco epidermal cells during the time window of the experiment (4-5 days).

Temperature rescue of X-ALD missense mutants

Although ALDP is an integral peroxisome membrane protein in wild type cells, in X-ALD patient cells, the majority of cases with missense mutations result in the absence or very marked reduction of ALDP from the membrane [56]. About 60 % of X-ALD *ABCD1* mutations are missense mutations, 65 % of which result in no detectable ALDP, based on immunofluorescence (IF), indicating that they affect protein folding and stability. We developed a method based on protein blot analysis for quantification of low amounts of ALDP (Fig. S2A) and reinvestigated these findings. Immunoblot analysis revealed that residual ALDP is present in all missense cell lines analysed, though sometimes below the level of detection by IF (Table 1; Fig. S2B). Protein was not present in the control line, which contains a frameshift mutation (p.Arg113fs). *ABCD1* RNA levels did not correlate well with levels of ALDP, suggesting that protein abundance is subject to post-transcriptional controls, consistent with the notion that missense X-ALD mutations affect protein folding and stability (Fig. S2B,C). A simple method to identify folding mutations is to lower the tissue culture temperature from 37°C to 30°C, allowing proteins more time to fold correctly and thus pass the quality control system. Therefore, X-ALD patient fibroblasts were cultured at 30°C, and the ALDP levels measured by quantitative immunoblotting. ALDP was not increased significantly in response to low temperature in 10 WT control lines tested (Fig. S3A), however, increased expression levels of ALDP were found in several of the X-ALD fibroblasts investigated, with the exception of p.Ser149Asn, Asp194His, pLeu220Pro p.Arg389His, p.Ser606Leu and p.His667Asp which did not exhibit a statistically significant increase (Fig. 4A,B). The effect of reduced temperature on *ABCD1* transcript abundance was variable, with no clear correlation to the effect on protein abundance (Fig. S3B).

We then examined whether ALDP function was rescued in selected cell lines which exhibited an increase in protein upon low-temperature culture. ALDP was increased from 2-4 % to ca. 20 % of WT levels in lines bearing the mutations p.Glu609Gly, p.Ala616Thr and p.Arg660Trp, from 1 to 10 % in p.Glu609Lys and p.Arg554His cells and from 45 to 75 % in the p.Asp194His line (Fig. 4A). VLCFA β-oxidation was measured in cells that were cultured at 30°C for 72 h, but in only one case (p.Ala616Thr) was the capacity to degrade VLCFA restored to near-control levels (Fig. 4C). However after four weeks' culture at 30 ºC, VLCFA levels were partially corrected in p.Arg660Trp, p.Arg554His and p.Ala616Thr fibroblasts. The apparent delay in alteration of VLCFA levels reflects slow turnover of VLCFA in fibroblasts, as demonstrated previously in a study in which the pharmacological agent 4-phenylbutyrate was used to correct β-oxidation and VLCFA levels in X-ALD cells [57]. Lines bearing the p.Glu609Gly and p.Asp194His mutations did not show any correction of the C26:0/C22:0 ratio (Fig. 4D). Lack of functional rescue may result if the missense mutation has a negative effect on ALDP transport activity or alternatively if the increased protein level upon low-temperature cultivation is not accompanied by correct targeting of ALDP.

X-ALD mutant proteins are expressed at the peroxisome in plant cells

Although we and others have shown that missense X-ALD mutations result in ALDP instability in mammalian cells (Fig. 4; [56, 58]), in a previous study, we noticed that *cts* mutants which have "protein-absent", disease-associated equivalents in human *ABCD1* were expressed as stable, correctly targeted proteins in Arabidopsis [46]. Therefore we tested whether ALDP variants bearing missense mutations which result in protein mis-targeting or instability in mammalian cells would behave similarly when expressed in plant cells. In addition to the temperature-sensitive mutants identified above, a range of X-ALD mutants with different intracellular fates was selected (Table 2; [58]), with the goal of comparing the capacity of plant and mammalian cells for sensing and turnover of defective peroxisomal membrane proteins. These included relatively common mutants which are unstable in fibroblasts but which can be rescued by the application of proteasome inhibitors (p.Ser606Leu, p.Arg617His, p.His667Asp), the p.Arg104Cys mutant in which degradation of ALDP cannot be prevented by proteasome inhibitors and the p.Tyr174Cys mutant which is mis-targeted in fibroblasts [58]. These mutations were introduced into the ALDP-YFP construct and transiently expressed in tobacco leaves which were stably transformed with CFP-SKL. In each case, the mutant proteins were detected in peroxisomes of tobacco epidermal cells, regardless of their intracellular fate in mammalian cells (Fig. 5 and Fig. S4). It is not possible to estimate protein turnover from transient transfection experiments, however, it is clear that the X-ALD proteins were targeted to the peroxisome in plant cells and that at least a proportion of the protein escaped proteasomal degradation, suggestive of increased stability. This points to differences in the sensing and turnover of defective PMPs in plants and animal cells.

We next considered whether the mutant forms of ALDP were more stable owing to the lower temperature at which plants are typically cultivated (ca. 22-25 ºC), compared to mammalian cells cultured at 37 ºC, by comparing the fates of X-ALD mutants which respond differently to low temperature rescue. ALDP proteins bearing p.Arg554His, p.Glu609Gly, p.Ala616Thr and p.Arg660Trp mutations are undetectable by immunofluorescence analysis of fibroblasts, but trace amounts are present, as revealed by immunoblotting (Table 1) and cultivation of fibroblasts at low temperature (30 ºC) leads to an increase in ALDP protein (Fig. 4A). In contrast, the ALDP level in p.His667Asp fibroblasts is not rescued by low temperature and X-ALD mutant p.Ser606Leu expresses IF-detectable ALDP at 37 ºC, with little increase upon low-temperature cultivation (Fig. 4A). Upon expression in tobacco epidermal cells, ALDP-YFP was observed in peroxisomes for each of these three classes of mutant, as judged by co-localisation with CFP-SKL (Fig. 5 and Fig. S4), suggesting that increased apparent stability of mutant ALDP in plant cells is not solely due to improved folding at lower temperature.

Differential ability of ALDP-YFP and ALDR-YFP to complement *cts-1*

Since ALDP and ALDR were correctly targeted when transiently expressed in tobacco leaves, we investigated whether the human *ABCD1* and *ABCD2* cDNAs could complement one or more of the different phenotypes of the Arabidopsis *cts-1* mutant. *cts-1* seeds are unable to germinate and complete seedling establishment but it is not clear whether the requirement of CTS for germination is related to the provision of energy and carbon skeletons from storage lipid catabolism, or due to the metabolism of a signal molecule by β-oxidation [29]. Therefore, two strategies were adopted to obtain plants homozygous for *cts-1* which stably expressed ABCD-YFP fusions. Firstly, homozygous *cts-1* plants were transformed directly and T1 seed were screened for the ability to germinate on 0.5 X MS medium plus antibiotic selection in the absence of exogenous sugars and mechanical disruption of the seed coat, both of which are required for the germination of *cts* seeds [26, 29]. Screening seeds from two independent transformations with 35S::ALDP-YFP or 35S::ALDR-YFP yielded no

transformants, suggesting either that these constructs did not complement the germination phenotype of *cts-1* and/or that they did not confer the ability to establish in the absence of exogenous sucrose. Thereafter, therefore, heterozygous plants (CTS/*cts-1*) were transformed with ALDP-YFP and T1 plants were identified by antibiotic selection and the genotypes confirmed by PCR (data not shown). These plants were allowed to self-fertilise and set seed; homozygous lines were obtained by inducing seeds to germinate by disrupting the seed coat and cultivating on medium containing sucrose. For ALDR-YFP, T1 transformants in the *cts-1* background were obtained by screening on medium containing antibiotics and sucrose.

The germination kinetics of homozygous lines expressing ALDP-YFP or ALDR-YFP in the *cts-1* background were compared with those of the corresponding wild type accession, L*er* and the untransformed mutant, *cts-1*. Seeds were placed on 0.5 x MS medium, dark-chilled for 2 d and then transferred to a growth cabinet for 7 d. After 7 d, >75 % of L*er* seeds had germinated, but no germination was observed for *cts-1* seeds or *cts-1* seeds expressing ALDP-YFP. In contrast to ALDP, >60% of *cts-1* seeds expressing ALDR-YFP germinated after 7 d (Fig. 6A; Fig, S5A). Expression of ALDR-YFP also repressed transcript levels of *ABI5*, a gene which has been proposed to inhibit germination in *cts* seeds [33] (Fig. S5B). However, development did not proceed further in the absence of sucrose, indicating that ALDR-YFP does not rescue the seedling establishment phenotype of *cts-1* (Fig. 6A).

To examine seedling establishment independently of germination, seeds expressing ALDP-YFP were placed on filters overlaid on 0.5 X MS medium containing sucrose and the seed coats gently disrupted with a needle. After 2 d dark chilling, plates were transferred to a growth chamber for 24 h to permit germination. Seeds were then transferred to medium lacking sucrose and returned to the growth chamber for a further 4-5 d. A duplicate plate was maintained on sucrose medium. After 5 days, L*er* seedlings had established (as judged by the presence of green cotyledons) on media with and without sucrose, but the *cts-1* mutant and *cts-1* lines expressing ALDP-YFP did not establish on media lacking sucrose (Fig. 6B). All genotypes were able to establish in the presence of 0.5 % sucrose (Fig. 6C), indicating that there were no deleterious effects associated with either transgene. To confirm correct targeting of ALDP, lines expressing ALDP-YFP were crossed to an Arabidopsis line stably expressing CFP-SKL [40] and the progeny examined by confocal microscopy. Punctate structures were observed in the YFP channel in hypocotyl cells; these coincided with peroxisomes visualised by CFP-SKL, indicating that ALDP-YFP is located in peroxisomes in Arabidopsis as well as in tobacco (Fig. S6A). ALDP-GFP was previously shown to be functional in fibroblasts [58], thus ruling out a negative effect of fusion to a fluorescent protein. The subcellular localisation of ALDR-YFP was tested by counterstaining with BODPIY 8, a YFP-compatible member of a series of BODIPY probes which target peroxisomes in plant cells [51]. The specificity of BODIPY 8 was confirmed using Arabidopsis plants stably expressing a YFP fusion of the peroxisomal protein, AtPex10 [40]. Co-localisation of BODIPY 8 with peroxisomes was observed, although not all organelles which stained with the probe were observed in the YFP channels, since the YFP bleached relatively rapidly and the signal was less intense than that of the dye (Fig. S6B). Co-localisation of the BODIPY signal and YFP in L*er* and *cts-1* plants expressing ALDR-YFP demonstrated peroxisomal targeting of this fusion protein in Arabidopsis (Fig. S6C,D).

The inability of *cts-1* lines expressing ALDP-YFP or ALDR-YFP to establish in the absence of exogenous sucrose suggests that they are unable to mobilise seed storage TAG which is required for growth before the seedlings become fully photosynthetic. Therefore the fatty acid contents of seedlings were determined by gas chromatographic analysis of fatty acid

methyl esters. As shown previously [26], *cts-1* seedlings retain TAG-derived fatty acids by comparison to WT, as judged by the increased level of eicosenoic acid (20:1), which is considered to be a marker for TAG in Arabidopsis [59] (Fig. 7). The *cts-1* mutant also exhibited a marked retention of C18 fatty acids and the VLCFA species, 20:0, 20:2 and 22:1. The fatty acid profiles of *cts-1*/ALDP-YFP and /ALDR-YFP seedlings were qualitatively and quantitatively similar to those of *cts-1*, confirming the inability of these transgenic lines to mobilise storage oil for the provision of carbon skeletons and energy during seedling establishment.

In WT plants, CTS is required for import of the pro-auxins, 2,4-dichlorophenoxybutyric acid (2,4-DB) and indole butyric acid (IBA) into the peroxisome where they are converted to bioactive auxins, 2,4-dichloroacetic acid (2,4-D) and indole acetic acid (IAA) respectively, by β-oxidation. *cts* mutants are unable to metabolise 2,4-DB and IBA and are therefore resistant to the growth inhibiting properties of these compounds [25, 27]. The ability of ALDP-YFP and ALDR-YFP to complement the 2,4-DB resistance phenotype of *cts-1* was tested: seeds were induced to germinate as described above and then transferred to plates containing 1 μM 2,4-DB or 30 μM IBA. Neither ALDP-YFP nor ALDR-YFP restored WT sensitivity to these compounds (Fig. 6D,E), indicating that the human peroxisomal ABC proteins were unable to mediate peroxisomal import of pro-auxins, in the transgenic lines analysed.

DISCUSSION

Peroxisomal ABC transporters are found in all eukaryotic kingdoms, but their domain organisation and the physiological context in which they operate varies. However, all have profound effects on the physiology of the organism when mutated. By testing the ability of ABCD family members to be correctly targeted and to complement phenotypes in a heterologous host [16, 17, 45, and this paper], we can begin to discern conserved and specialised functions.

In this paper, we show that ABCD family targeting is conserved between the plant and animal kingdom, but protein quality control differs. Several studies have reported that various ALDP missense mutants do not produce protein in human fibroblasts, however we demonstrated that protein is present at low levels and protein levels of a subset of mutants can be increased by low-temperature culture. In some cases, this led to partial recovery of function. The potential utility of these findings clearly depends on the effect of a given mutation on ALDP function, but this opens up the possibility for therapeutic intervention aimed at stabilising and promoting the correct targeting of selected missense mutations using chemical chaperones. In plants however, all the X-ALD mutants were correctly targeted, regardless of their fate in fibroblasts. The mechanistic basis for this finding remains to be explored; however, it may have important implications for expression of heterologous membrane proteins in plants.

ALDP could not complement the germination or establishment phenotypes of *cts-1* but ALDR could complement the germination phenotype. The failure to complement establishment is not surprising, given the reported substrate specificity of ALDP and ALDR [16, 17]. This separation of physiological function provides additional evidence to support the assertion that the processes of germination and establishment are biochemically distinct [29]. Conversely, the ability of CTS to support beta-oxidation of a wide range of fatty acids in

yeast points to a broad substrate specificity [34], whereas the mammalian ABCDs have much more restricted substrates (this study and [16, 17]).

ACKNOWLEDGEMENTS

We gratefully acknowledge Dr Gareth Howell and Dr Laura-Anne Brown for advice and assistance with the microscopy and Dr Fred Beaudoin for guidance with fatty acid analysis of seedlings. We thank Barbara Johnson for maintenance of tobacco lines, Professor Johannes Berger for ALDP/pcDNA3.1, Stephen Parsons for ALDP/pDONR207, Dr. Jurgen Deneke for GFP-HDEL seeds and Drs Patrick Steel and Andrei Smertenko for generously providing BODIPY 8.

FUNDING

This research was supported by BBSRC grants BB/F007108/1 to FLT and BB/F007299/1 to AB/SAB and a grant from the Netherlands Organization for Scientific Research (VIDI-grant No. 91786328) to SK and the EU grant (FP7 LEUKOTREAT 241622) to SK. Rothamsted Research receives grant-aided support from the BBSRC of the UK.

REFERENCES

1. Wanders, R.J. (2004) Peroxisomes, lipid metabolism, and peroxisomal disorders. Mol Genet Metab. **83**, 16-27
2. Schumann, U., Wanner, G., Veenhuis, M., Schmid, M. and Gietl, C. (2003) AthPEX10, a nuclear gene essential for peroxisome and storage organelle formation during Arabidopsis embryogenesis. Proc Natl Acad Sci U S A. **100**, 9626-9631
3. Sparkes, I.A., Brandizzi, F., Slocombe, S.P., El-Shami, M., Hawes, C. and Baker, A. (2003) An Arabidopsis *pex10* null mutant is embryo lethal, implicating peroxisomes in an essential role during plant embryogenesis. Plant Physiol. **133**, 1809-1819
4. Fan, J., Quan, S., Orth, T., Awai, C., Chory, J. and Hu, J. (2005) The Arabidopsis PEX12 gene is required for peroxisome biogenesis and is essential for development. Plant Physiol. **139**, 231-239
5. Nito, K., Kamigaki, A., Kondo, M., Hayashi, M. and Nishimura, M. (2007) Functional classification of Arabidopsis peroxisome biogenesis factors proposed from analyses of knockdown mutants. Plant Cell Physiol. **48**, 763-774.
6. Kemp, S. and Wanders, R.J. (2007) X-linked adrenoleukodystrophy: very long-chain fatty acid metabolism, ABC half-transporters and the complicated route to treatment. Mol Genet Metab. **90**, 268-276
7. Kemp, S. and Wanders, R. (2010) Biochemical aspects of X-linked adrenoleukodystrophy. Brain Pathol. **20**, 831-837.
8. Mosser, J., Douar, A.M., Sarde, C.O., Kioschis, P., Feil, R., Moser, H., Poustka, A.M., Mandel, J.L. and Aubourg, P. (1993) Putative X-linked adrenoleukodystrophy gene shares unexpected homology with ABC transporters. Nature. **361**, 726-730
9. Rottensteiner, H. and Theodoulou, F.L. (2006) The ins and outs of peroxisomes: co-ordination of membrane transport and peroxisomal metabolism. Biochim Biophys Acta **1763**, 1527-1540
10. Higgins, C.F. (1992) ABC transporters: from microorganisms to man. Annu Rev Cell Biol. **8**, 67-113

11. Kemp, S., Theodoulou, F.L. and Wanders, R.J.A. (2011) Mammalian peroxisomal ABC transporters. Br J Pharmacol., *submitted*.
12. Hettema, E.H., van Roermund, C.W., Distel, B., van den Berg, M., Vilela, C., Rodrigues-Pousada, C., Wanders, R.J. and Tabak, H.F. (1996) The ABC transporter proteins Pat1 and Pat2 are required for import of long-chain fatty acids into peroxisomes of *Saccharomyces cerevisiae*. EMBO J. **15**, 3813-3822
13. Shani, N. and Valle, D. (1996) A *Saccharomyces cerevisiae* homolog of the human adrenoleukodystrophy transporter is a heterodimer of two half ATP-binding cassette transporters. Proc Natl Acad Sci U S A. **93**, 11901-11906
14. Verleur, N., Hettema, E.H., van Roermund, C.W., Tabak, H.F. and Wanders, R.J. (1997) Transport of activated fatty acids by the peroxisomal ATP-binding-cassette transporter Pxa2 in a semi-intact yeast cell system. Eur J Biochem. **249**, 657-661
15. Ofman, R., Dijkstra, I.M., van Roermund, C.W., Burger, N., Turkenburg, M., van Cruchten, A., van Engen, C.E., Wanders, R.J. and Kemp, S. (2010) The role of ELOVL1 in very long-chain fatty acid homeostasis and X-linked adrenoleukodystrophy. EMBO Mol Med. **2**, 90-97
16. van Roermund, C.W., Visser, W.F., Ijlst, L., van Cruchten, A., Boek, M., Kulik, W., Waterham, H.R. and Wanders, R.J. (2008) The human peroxisomal ABC half transporter ALDP functions as a homodimer and accepts acyl-CoA esters. FASEB J. **22**, 4201-4208
17. van Roermund, C.W., Visser, W., Ijlst, L., Waterham, H.R. and Wanders, R.J.A. (2011) Differential substrate specificities of human ABCD1 and ABCD2 in peroxisomal fatty acid β-oxidation. Biochim Biophys Acta, **1811**, 148-152
18. Fourcade, S., Ruiz, M., Camps, C., Schlüter, A., Houten, S.M., Mooyer, P.A., Pàmpols, T., Dacremont, G., Wanders, R.J., Giròs, M. and Pujol, A. (2009) A key role for the peroxisomal ABCD2 transporter in fatty acid homeostasis. Am J Physiol Endocrinol Metab. **296**, E211-21.
19. Genin, E., Geillon, F., Gondecaille, C., Athias, A., Gambert, P., Trompier, D. and Savary, S. (2011) Substrate specificity overlap and interaction between Adrenoleukodystrophy protein (ALDP/ABCD1) and Adrenoleukodystrophy-related protein (ALDRP/ABCD2). J Biol Chem. *in press*.
20. Braiterman, L.T., Zheng, S., Watkins, P.A., Geraghty, M.T., Johnson, G., McGuinness, M.C., Moser, A.B. and Smith, K.D. (1998) Suppression of peroxisomal membrane protein defects by peroxisomal ATP binding cassette (ABC) proteins. Hum Mol Genet. **7**, 239-247
21. Netik, A., Forss-Petter, S., Holzinger, A., Molzer, B., Unterrainer, G. and Berger, J. (1999) Adrenoleukodystrophy-related protein can compensate functionally for adrenoleukodystrophy protein deficiency (X-ALD): implications for therapy. Hum Mol Genet. **8**, 907-913
22. Di Benedetto, R., Denti, M.A., Salvati, S., Sanchez, M., Attorri, L., David, G. and Di Biase, A. (2008) RNAi-mediated silencing of ABCD3 gene expression in rat C6 glial cells: a model system to study PMP70 function. Neurochem Int. **52**, 1106-1113
23. Wanders, R.J., Vreken, P., Ferdinandusse, S., Jansen, G.A., Waterham, H.R., van Roermund, C.W. and van Grunsven, E.G. (2001) Peroxisomal fatty acid alpha- and beta-oxidation in humans: enzymology, peroxisomal metabolite transporters and peroxisomal diseases. Biochem Soc Trans. **29**, 250-67
24. Kashiwayama, Y., Seki, M., Yasui, A., Murasaki, Y., Morita, M., Yamashita, Y., Sakaguchi, M., Tanaka, Y. and Imanaka, T. (2009) 70-kDa peroxisomal membrane protein related protein (P70R/ABCD4) localizes to endoplasmic reticulum not

peroxisomes, and NH2-terminal hydrophobic property determines the subcellular localization of ABC subfamily D proteins. Exp Cell Res. **315**, 190-205
25. Zolman, B.K., Silva, I.D. and Bartel, B. (2001) The Arabidopsis *pxa1* mutant is defective in an ATP-binding cassette transporter-like protein required for peroxisomal fatty acid beta-oxidation. Plant Physiol. **127**, 1266-1278
26. Footitt, S., Slocombe, S.P., Larner, V., Kurup, S., Wu, Y., Larson, T., Graham, I., Baker, A. and Holdsworth, M. (2002) Control of germination and lipid mobilization by COMATOSE, the Arabidopsis homologue of human ALDP. EMBO J. **21**, 2912-2922
27. Hayashi, M., Nito, K., Takei-Hoshi, R., Yagi, M., Kondo, M., Suenaga, A., Yamaya, T. and Nishimura, M. (2002) Ped3p is a peroxisomal ATP-binding cassette transporter that might supply substrates for fatty acid beta-oxidation. Plant Cell Physiol. **43**, 1-11
28. Hooks, M.A., Turner, J.E., Murphy, E.C., Johnston, K.A., Burr, S. and Jarosławski, S. (2007) The Arabidopsis ALDP protein homologue COMATOSE is instrumental in peroxisomal acetate metabolism. Biochem J. **406**, 399-406
29. Footitt, S., Marquez, J., Schmuths, H., Baker, A., Theodoulou, F.L. and Holdsworth, M. (2006) Analysis of the role of COMATOSE and peroxisomal beta-oxidation in the determination of germination potential in Arabidopsis. J Exp Bot. **57**, 2805-2814
30. Footitt, S., Dietrich, D., Fait, A., Fernie, A.R., Holdsworth, M.J., Baker, A. and Theodoulou, F.L. (2007) The COMATOSE ATP-binding cassette transporter is required for full fertility in Arabidopsis. Plant Physiol. **144**, 1467-1480
31. Kunz, H.H., Scharnewski, M., Feussner, K., Feussner, I., Flügge, U.I., Fulda, M. and Gierth, M. (2009) The ABC transporter PXA1 and peroxisomal beta-oxidation are vital for metabolism in mature leaves of Arabidopsis during extended darkness. Plant Cell. **21**, 2733-2749
32. Slocombe, S.P., Cornah, J., Pinfield-Wells, H., Soady, K., Zhang, Q., Gilday, A., Dyer, J.M. and Graham, I.A. (2009) Oil accumulation in leaves directed by modification of fatty acid breakdown and lipid synthesis pathways. Plant Biotechnol J. **7**, 694-703
33. Kanai, M., Nishimura, M. and Hayashi, M. (2010) A peroxisomal ABC transporter promotes seed germination by inducing pectin degradation under the control of ABI5. Plant J. **62**, 936-947
34. Nyathi, Y., De Marcos Lousa, C., van Roermund, C.W., Wanders, R.J., Johnson, B., Baldwin, S.A., Theodoulou, F.L. and Baker, A. (2010) The Arabidopsis peroxisomal ABC transporter, comatose, complements the *Saccharomyces cerevisiae pxa1 pxa2Δ* mutant for metabolism of long-chain fatty acids and exhibits fatty acyl-CoA-stimulated ATPase activity. J Biol Chem. **285**, 29892-29902
35. Theodoulou, F.L., Job, K., Slocombe, S.P., Footitt, S., Holdsworth, M., Baker, A., Larson, T.R. and Graham, I.A. (2005) Jasmonic acid levels are reduced in COMATOSE ATP-binding cassette transporter mutants. Implications for transport of jasmonate precursors into peroxisomes. Plant Physiol. **137**, 835-840
36. Girzalsky, W., Saffian, D. and Erdmann, R. (2010) Peroxisomal protein translocation. Biochim Biophys Acta. **1803**, 724-731
37. Schmidt, F., Treiber, N., Zocher, G., Bjelic, S., Steinmetz, M.O., Kalbacher, H., Stehle, T. and Dodt, G. (2010) Insights into peroxisome function from the structure of PEX3 in complex with a soluble fragment of PEX19. J Biol Chem. **285**, 25410-25417
38. Schueller, N., Holton, S.J., Fodor, K., Milewski, M., Konarev, P., Stanley, W.A., Wolf, J., Erdmann, R., Schliebs, W., Song, Y.H. and Wilmanns, M. (2010) The peroxisomal receptor Pex19p forms a helical mPTS recognition domain. EMBO J. **29**, 2491-2500

39. Strausberg, R.L., Feingold, E.A., Grouse, L.H., Derge, J.G., Klausner, R.D., Collins, F.S., Wagner, L., Shenmen, C.M., Schuler, G.D., Altschul, S.F., *et al*. (2002) Generation and initial analysis of more than 15,000 full-length human and mouse cDNA sequences. Proc. Natl. Acad. Sci. USA. **99**, 16899-16903
40. Sparkes, I.A., Hawes, C. and Baker, A. (2005) AtPEX2 and AtPEX10 are targeted to peroxisomes independently of known endoplasmic reticulum trafficking routes. Plant Physiol. **139**, 690-700
41. Hadden, D.A., Phillipson, B.A., Johnston, K.A., Brown, L.A., Manfield, I.W., El-Shami, M., Sparkes, I.A. and Baker, A. (2006) Arabidopsis PEX19 is a dimeric protein that binds the peroxin PEX10. Mol Membr Biol. **23**, 325-336
42. Boisnard-Lorig, C., Colon-Carmona, A., Bauch, M., Hodge, S., Doerner, P., Bancharel, E., Dumas, C., Haseloff, J. and Berger, F. (2001) Dynamic analyses of the expression of the HISTONE::YFP fusion protein in Arabidopsis show that syncytial endosperm is divided in mitotic domains. Plant Cell. **13**, 495-509
43. Unterrainer, G., Molzer, B., Forss-Petter, S. and Berger, J. (2000) Co-expression of mutated and normal adrenoleukodystrophy protein reduces protein function: implications for gene therapy of X-linked adrenoleukodystrophy. Hum Mol Genet. **9**, 2609-2616
44. Sparkes, I.A., Runions, J., Kearns, A. and Hawes, C. (2006) Rapid, transient expression of fluorescent fusion proteins in tobacco plants and generation of stably transformed plants. Nat Protoc. **1**, 2019-2025
45. Clough, S.J. and Bent, A.F. (1998) Floral dip: a simplified method for Agrobacterium-mediated transformation of *Arabidopsis thaliana*. Plant J. **16**, 735-743
46. Dietrich, D., Schmuths, H., De Marcos Lousa, C., Baldwin, J.M., Baldwin, S.A., Baker, A., Theodoulou, F.L. and Holdsworth, M.J. (2009) Mutations in the Arabidopsis peroxisomal ABC transporter COMATOSE allow differentiation between multiple functions *in planta*: insights from an allelic series. Mol Biol Cell. **20**, 530-543
47. Linka, N., Theodoulou, F.L., Haslam, R.P., Linka, M., Napier, J.A., Neuhaus, H.E. and Weber, A.P. (2008) Peroxisomal ATP import is essential for seedling development in *Arabidopsis thaliana*. Plant Cell. **20**, 3241-32
48. Engelen, M., Ofman, R., Mooijer, P.A., Poll-The, B.T., Wanders, R.J. and Kemp, S. (2008) Cholesterol-deprivation increases mono-unsaturated very long-chain fatty acids in skin fibroblasts from patients with X-linked adrenoleukodystrophy. Biochim Biophys Acta. **1781**, 105-111
49. Kemp, S., Valianpour, F., Mooyer, P.A., Kulik, W. and Wanders, R.J. (2004) Method for measurement of peroxisomal very-long-chain fatty acid beta-oxidation in human skin fibroblasts using stable-isotope-labeled tetracosanoic acid. Clin Chem. **50**, 1824-1826
50. Valianpour, F., Selhorst, J.J., van Lint, L.E., van Gennip, A.H., Wanders, R.J. and Kemp, S. (2003) Analysis of very long-chain fatty acids using electrospray ionization mass spectrometry. Mol Genet Metab. **79**, 189-196
51. Landrum, M., Smertenko, A., Edwards, R., Hussey, P.J. and Steele, P.G. (2010) BODIPY probes to study peroxisome dynamics *in vivo*. Plant J. **62**, 529-538
52. Halbach, A., Lorenzen, S., Landgraf, C., Volkmer-Engert, R., Erdmann, R. and Rottensteiner, H. (2005) Function of the PEX19-binding site of human adrenoleukodystrophy protein as targeting motif in man and yeast. PMP targeting is evolutionarily conserved. J Biol Chem. **280**, 21176-21182

53. Yernaux, C., Fransen, M., Brees, C., Lorenzen, S. and Michels, P.A. (2006) *Trypanosoma brucei* glycosomal ABC transporters: identification and membrane targeting. Mol Membr Biol. **23**, 157-172
54. Saveria, T., Halbach, A., Erdmann, R., Volkmer-Engert, R., Landgraf, C., Rottensteiner, H. and Parsons, M. (2007) Conservation of PEX19-binding motifs required for protein targeting to mammalian peroxisomal and trypanosome glycosomal membranes. Eukaryot Cell. **6**, 1439-1449
55. Sacksteder, K.A., Jones, J.M., South, S.T., Li, X., Liu, Y. and Gould, S.J. (2000) PEX19 binds multiple peroxisomal membrane proteins, is predominantly cytoplasmic, and is required for peroxisome membrane synthesis. J Cell Biol. **148**, 931-944
56. Kemp, S., Pujol, A., Waterham, H.R., van Geel, B.M., Boehm, C.D., Raymond, G.V., Cutting, G.R., Wanders, R.J. and Moser, H.W. (2001) ABCD1 mutations and the X-linked adrenoleukodystrophy mutation database: role in diagnosis and clinical correlations. Hum Mutat. **18,** 499-515
57. Kemp, S., Wei, H.M., Lu, J.F., Braiterman, L.T., McGuinness, M.C., Moser, A.B., Watkins, P.A., and Smith, K.D. (1998) Gene redundancy and pharmacological gene therapy: implications for X-linked adrenoleukodystrophy. Nat Med. **4**, 1261-1268
58. Takahashi, N., Morita, M., Maeda, T., Harayama, Y., Shimozawa, N., Suzuki, Y., Furuya, H., Sato, R., Kashiwayama, Y. and Imanaka, T. (2007) Adrenoleukodystrophy: subcellular localization and degradation of adrenoleukodystrophy protein (ALDP/ABCD1) with naturally occurring missense mutations. J Neurochem. **101**, 1632-1643
59. Lemieux, B., Miquel, M., Somerville, C., and Browse, J. (1990) Mutants of Arabidopsis with alterations in seed lipid fatty-acid composition. Theor. Appl. Genet. **80**, 234-240

FIGURE LEGENDS

Figure 1. Targeting of mammalian ABCD-YFP fusions in plant cells
(A-C) Tobacco plants stably expressing CFP-SKL were transiently transfected with constructs containing ABCD-YFP fusions driven by the cauliflower mosaic virus 35S promoter. Leaf epidermal cells were imaged using confocal microscopy; from left to right: CFP, YFP, bright field and merge. A, ALDP; B, ALDR; C, PMP70. Panel D: tobacco plants stably expressing GFP-HDEL were transiently transfected with 35S::ABCD4(P70R/PMP69)-YFP. Left to right: GFP, YFP, bright field and merge. Scale bars 10 µm. Images are representative of results from at least three independent experiments.

Figure 2. Interaction of mammalian ABCD proteins with Arabidopsis Pex19 *in vitro*
AtPex19_1 was expressed as a GST fusion protein in *E.coli*. Purified GST-AtPex19-1 (or GST only, negative control) was immobilised on glutathione beads and incubated with *in vitro* translated peroxisomal ABC transporters labelled with BODIPY-lysine. Interacting proteins were eluted with SDS-PAGE buffer and separated in a 12 % acrylamide denaturing gel. Labelled proteins were visualised by fluorography. 20 % input, 20 % of the ABCD proteins used in the pull-down experiment; GST, pull-down with GST alone; GST-AtPex19, pull-down with GST-AtPex19_1. Figures at the left hand side of the panel indicate the position of molecular weight markers (kDa). Results are representative of three independent experiments.

Figure 3. Interaction of mammalian ABCD proteins with Arabidopsis Pex19 *in vivo*

Tobacco plants stably expressing CFP-SKL were co-transfected with 35S::ABCD-YFP fusions and NLS-Pex19 constructs. Leaf epidermal cells were imaged using confocal microscopy: (A-D) ALDP-YFP plus NLS-HsPex19; (E-H) ALDP-YFP plus NLS-AtPex19_1; (I-J) ALDR-YFP plus NLS-AtPex19_1. (A,E,I) CFP; (B,F,J) YFP; (C,G,K) bright field; (D,H,L) merge. Scale bars: 10 µm. Results are representative of three independent experiments.

Figure 4. Low-temperature rescue of X-ALD fibroblasts

(A) ALDP expression levels in fibroblasts bearing X-ALD missense mutations, cultured at 37°C and at 30°C for 7 d. Asterisks indicate statistically significant differences, as determined by an unpaired t-test (* = $P < 0.05$, ** = $P < 0.01$, *** = $P < 0.001$). (B) Representative western blot, showing increase in ALDP in selected fibroblasts following culture at 30°C for 7 d. (C) VLCFA β-oxidation capacity in control fibroblasts from two different individuals and missense mutant ALDP-expressing fibroblasts cultured at 37°C or at 30°C for 3 d. Values are means ± SD; n=3. (D) Ratio of C26:0/C22:0 in control fibroblasts and missense mutant ALDP expressing fibroblasts cultured at 30°C for the time indicated. Values are means ± SD; n=3.

Figure 5. Targeting of missense X-ALD mutants in plant cells

Tobacco plants stably expressing CFP-SKL were transfected with 35S::ABCD-YFP fusions bearing X-ALD mutations reported in [58] and in this study (Fig. 4): p.Arg104Cys, p.Tyr174Cys, p.Ser606Leu, p.Ala616Thr, p.His667Asp. Leaf epidermal cells were imaged using confocal microscopy. (A) CFP (B) YFP (C) bright field (D) merge. Scale bars: 10 µm. Images are representative of results from three independent experiments.

Figure 6. Expression of ALDP-YFP and ALDR-YFP in *cts-1*

(A) Germination and subsequent seedling establishment of wild type (L*er*), *cts-1*, and *cts-1* transgenic lines expressing ALDP-YFP and ALDR-YFP. Images were recorded after 5 d on 0.5 X MS medium. Note the radicle emergence in *cts-1*/ALDR. (B) Seedling establishment analysed independently of germination: *cts-1* and *cts-1*/ALDP seeds were induced to germinate by mechanical disruption of the seed coat and growth for one day on 0.5 X MS medium containing 1 % (w/v) sucrose, then transferred to 0.5 X MS medium for a further 4 d (C-E) Growth of seedlings on 0.5 X MS medium containing 1 % (w/v) sucrose. *cts-1* and *cts-1*/ALDP-YFP seeds were induced to germinate by mechanical disruption of the seed coat. (C) no addition; (D) 1 µM 2,4-DB, (E) 30 µM IBA. Scale bar: 5 mm. Inset panels in (A) show seeds magnified 10 times. Results are representative of several independent transgenic lines.

Figure 7. Fatty acid profile of seedlings expressing mammalian ABCD transporters

Seedlings were cultured for 5 d on 0.5 X MS medium containing 1 % (w/v) sucrose. *cts-1* and *cts-1*/ALDP-YFP seeds were induced to germinate by mechanical disruption of the seed coat. Fatty acid methyl esters were determined for whole seedlings. Bars represent means ± SD (n =3).

Table 1. Quantification of ALDP levels in X-ALD fibroblasts

Mutation	ALDP	
	Immunofluorescence	**Immunoblot (% control)**
p.Arg74Trp	Absent	7.5 ± 0.6
p.Arg104Cys	Reduced	35 ± 3.0
p.Ser149Asn	Present	77 ± 3.0
p.Asp194His	Present	60 ± 13.6
p.Leu220Pro	Reduced	21.8 ± 5.4
p.Arg389His	Present	40.6 ± 3.6
p.Arg554His	Absent	1.0 ± 0.5
p.Ser606Leu	Present	25 ± 1.5
p.Glu609Gly	Absent	2.1 ± 1.3
p.Glu609Lys	Absent	1.8 ± 0.9
p.Ala616Thr	Absent	4.3 ± 1.7
p.Leu654Pro	Absent	1.5 ± 1.3
p.Arg660Trp	Absent	1.6 ± 0.8
p.His667Asp	Absent	2.9 ± 1.0
p.Arg113fs	Absent	-

Table 2. X-ALD mutants used for analysis of targeting in tobacco cells

X-ALD mutation	position	Protein fate in fibroblasts/CHO cells	Occurrence[a]
p.Arg104Cys	TMD1	Degraded in CHO cells, no MG-132 rescue[1]. Protein increased by low temperature.[2]	n=6, protein reduced/absent
p.Tyr174Cys	3 residues upstream of coupling helix 1	Mistargeted[1]	n=12, protein absent
p.Arg554His	NBD, 3 residues downstream of Q loop	Protein absent, rescued by low temperature. [2]	n=25, protein absent
p.Ser606Leu	NBD, ABC motif	Degraded, rescued by MG-132[1]; little effect of low temperature.[2]	n=12, protein present (p.Ser606Pro; n=3, absent)
p.Glu609Gly	NBD, ABC motif	Protein absent, increased by low temperature; no functional rescue.[2]	n=1 protein absent (p.Glu609Lys; n=14, absent)
p.Ala616Thr	NBD, between ABC and Walker B	Protein absent, rescued by low temperature.[2]	n=1, protein absent
p.Arg617His	NBD, between ABC and Walker B	Degraded, rescued by MG-132[1]	n=20, protein absent
p.Arg660Trp	NBD, H-loop	Protein absent, rescued by low temperature.[2]	n=18, protein absent
p.His667Asp	NBD, 5 residues downstream of H-loop	Degraded, rescued by MG-132[1]; little effect of low temperature.[2]	n=3, protein absent

a. Number of documented patients bearing the mutation; source: X-ALD database (www.x-ald.nl)
References: (1) [58]; (2) this study.
Abbreviations: TMD, transmembrane domain; NBD, nucleotide binding domain.

Table S1. Primers used for plasmid construction

Primer	Sequence
	Primers for plant expression constructs
ABCD1attB1	GGGGACAAGTTTGTACAAAAAAGCAGGCTAACAATGGCTCCGGTGCTCTCCA
ABCD1attB2	GGGGACCACTTTGTACAAGAAAGCTGGGTAGGTGGAGGCACCCTGGAG
ABCD2attB1	GGGGACAAGTTTGTACAAAAAAGCAGGCTAACAATGACACATATGCTAAATGC
ABCD2attB2	GGGGACCACTTTGTACAAGAAAGCTGGGTAAGATGTCTCATCTTCATTTTT
ABCD3attB1	GGGGACAAGTTTGTACAAAAAAGCAGGCTAACAATGGCGGCCTTCAGCAAG
ABCD3attB2	GGGGACCACTTTGTACAAGAAAGCTGGGTATGATCCGAACTCAACTG
ABCD4attB1	GGGGACAAGTTTGTACAAAAAAGCAGGCTAACAATGGCGGTCGCGGGGCCC
ABCD4attB2	GGGGACCACTTTGTACAAGAAAGCTGGGTATTCCACTTTGATTCTCATC
	NLS construct primers
AtPex19SalIFor	GGAGCTGGAGTCGACGCGAACAGTCACACCGAT
AtPex19SacIIRev	GGAGCTGGACCGCGGTCACATGATACAGCAATT
H2BSalIFor	GGAGCTGGAGTCGACATGGCGAAGGCAGATAAG
H2BXhoIRev	GGAGCTGGACTCGAGTCCAGCTCCAGCAGAACTC
H2BAtPex19attB1	GGGGACAAGTTTGTACAAAAAAGCAGGCTAACAATGGCGAAGGCAGATAAG
H2BAtPex19attB2	GGGGACCACTTTGTACAAGAAAGCTGGGTATCACATGATACAGCAATTTGG
	Primers for GST fusion and *in vitro* translation constructs
FT119	GAGGATCCATGGCGAACAGTCACACC
FT120	CTGCGGCCGCTCACATGATACAGC
FT121	GAGTCGACATGGCCAACGATAC
FT122	CTGCGGCCGCTCACATTACACAACA
FT123	GAGGATCCATGGCCGCCGCTGAGG
FT124	CTGCGGCCGCTCACATGATCAGACAC
FT125	CA**GGATCC**ACCATGACACATATGCTAAATGC
FT126	CG**TCTAGA**TTAAGATGTCTCATC
FT127	CA**GGATCC**ACCATGGCGGCCTTCAGC
FT128	GC**TCTAGA**CTATGATCCGAACTC
	Primers for site-directed mutagenesis
R104L for	CGGCCGCCTTGGTGAGCCTCACCTTCCTGTCGGTGTA
R104L rev	TACACCGACAGGAAGGTGAGGCTCACCAAGGCGGCCG
Y174C for	GCCTACCGCCTCTGCTCCTCCCAG
Y174C rev	CTGGGAGGAGCAGAGGCGGTAGGC
R554H for	CATGTCTGTGGGCTCCCTGCATGACCAGGTGATCTACCCGG

R554H rev	CCGGGTAGATCACCTGGTCATGCAGGGAGCCCACAGACATG
S606L for	AAGGACGTCCTGTTGGGTGGCGAGAAG
S606L rev	CTTCTCGCCACCCAACAGGACGTCCTT
E609G for	GACGTCCTGTCGGGTGGCGGGAAGCAGAGAATCGGCATG
E609G rev	CATGCCGATTCTCTGCTTCCCGCCACCCGACAGGACGTC
A616T for	GAAGCAGAGAATCGGCATGACCCGCATGTTCTACCACAG
A616T rev	CTGTGGTAGAACATGCGGGTCATGCCGATTCTCTGCTTC
R617H for	GCAGAGAATCGGCATGGCCCACATGTTCTACCACAGGC
R617H rev	GCCTGTGGTAGAACATGTGGGCCATGCCGATTCTCTGC
R660W for	CCCTGCTCTCCATCACCCACTGGCCCTCCCTGTGGAAATAC
R660W rev	GTATTTCCACAGGGAGGGCCAGTGGGTGATGGAGAGCAGGG
H667D for	TCCCTGTGGAAATACGACACACACTTGCTA
H667D rev	TAGCAAGTGTGTGTCGTATTTCCACAGGGA
	Primers for quantitative RT-PCR of *ABCD1* mRNA
ABCD1 for	CGTGGCTGTGACTTCCTACA
ABCD1 rev	AGGCGCTCCACACATACTTC
PPIB for	TGGAGAGCACCAAGACAGACA
PPIB rev	CTTCTCCACCTCGATCTTGC
	Primers for quantitative RT-PCR of *ABI5* mRNA
ABI5for	TAGAGGTGGTGGTAGCGGTAAT
ABI5rev	GCTTCGGGTTTGGATTAGGT
18SrRNAfor	ACGCTCCTGGTCTTAATTGG
18SrRNAreve	TCATTACTCCGATCCCGAAG
GAPDHfor	GCCATCCCTCAATGGAAAATT
GAPDHrev	GAGACATCAACGGTTGGAACA

Fig. 1

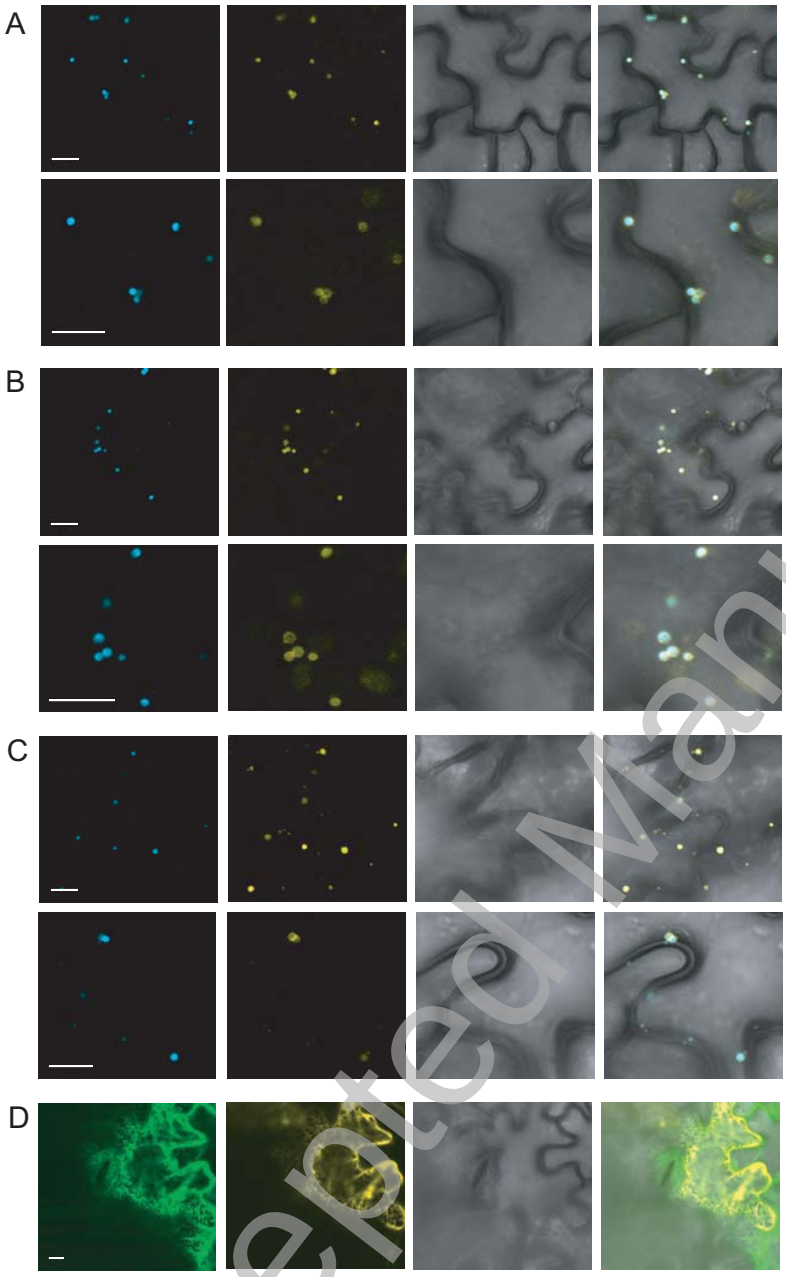

Fig. 2

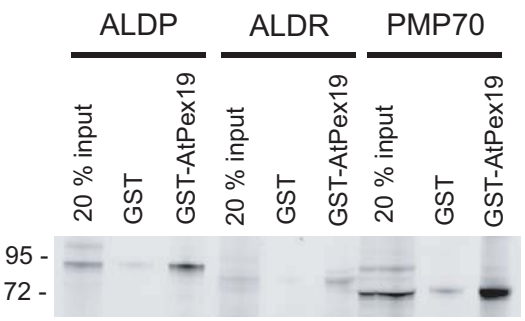

Fig. 3

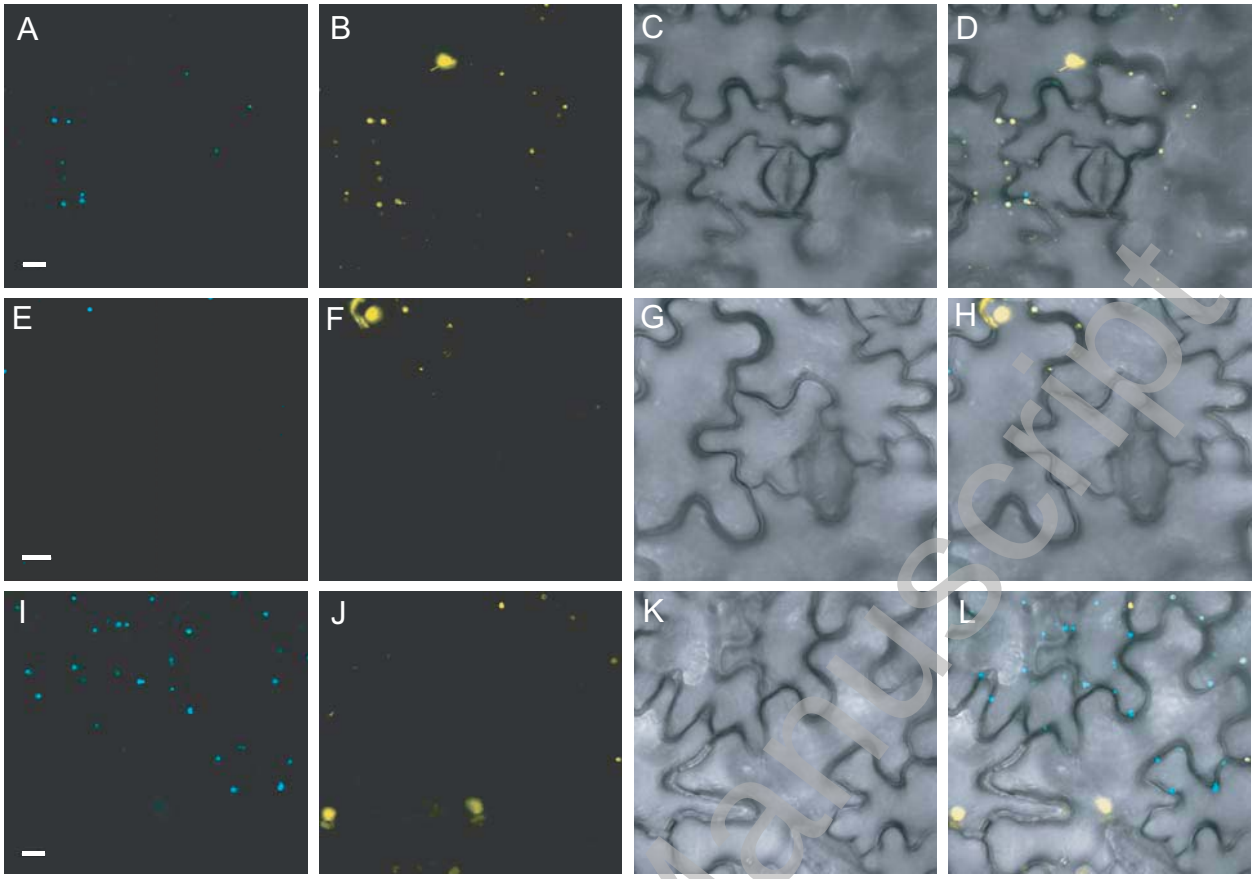

Fig. 4

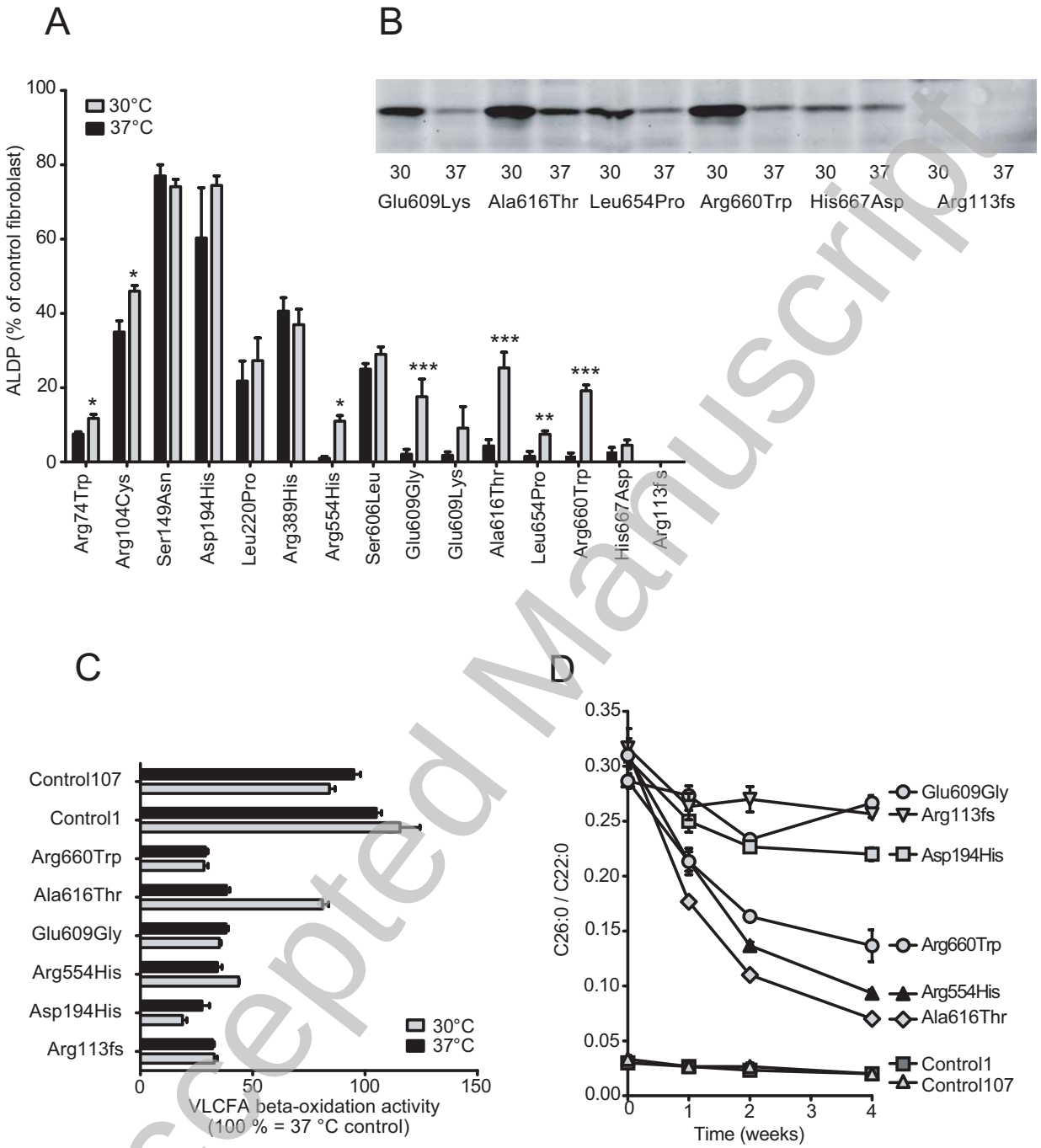

Fig. 5

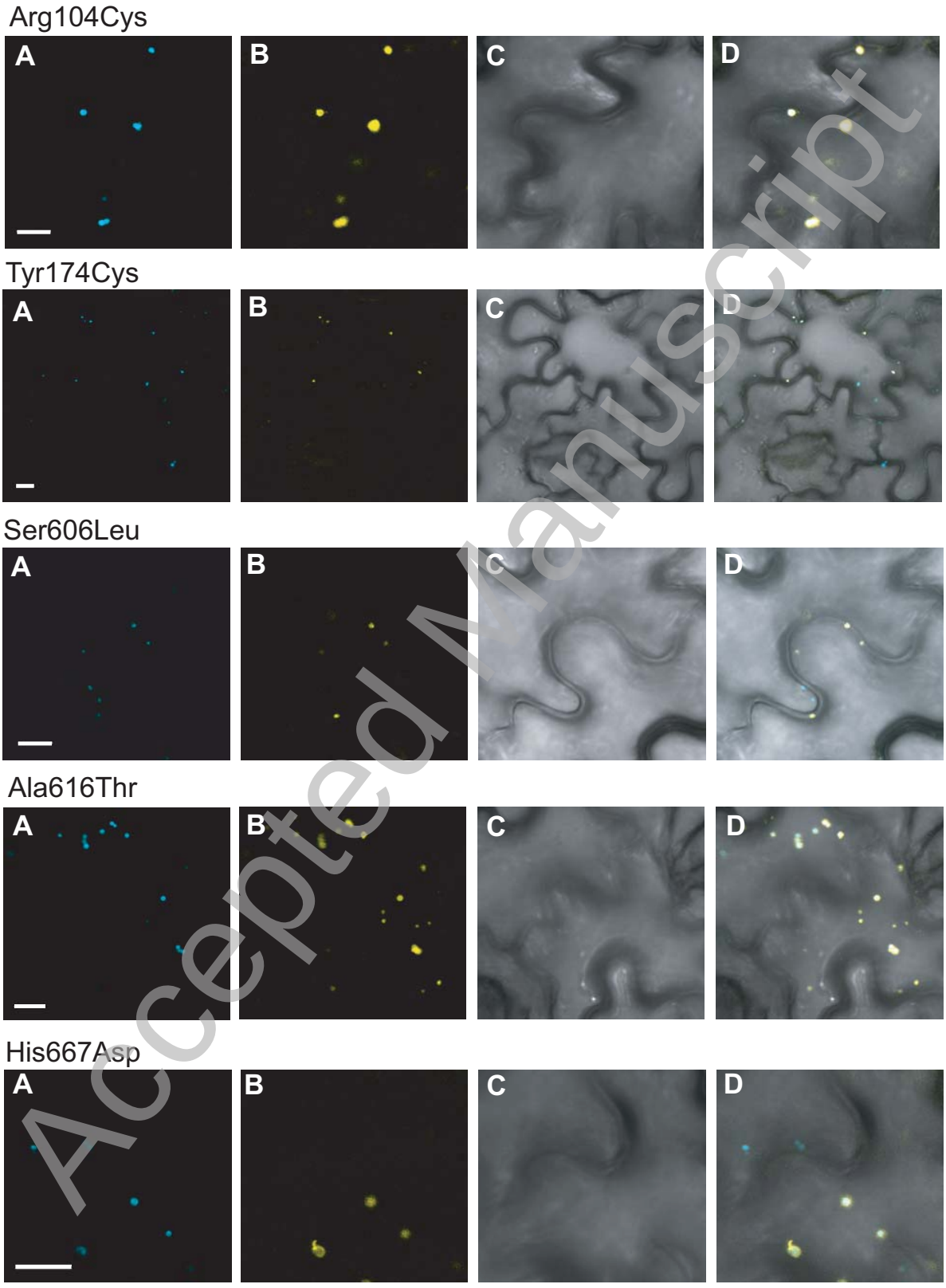

Fig. 6

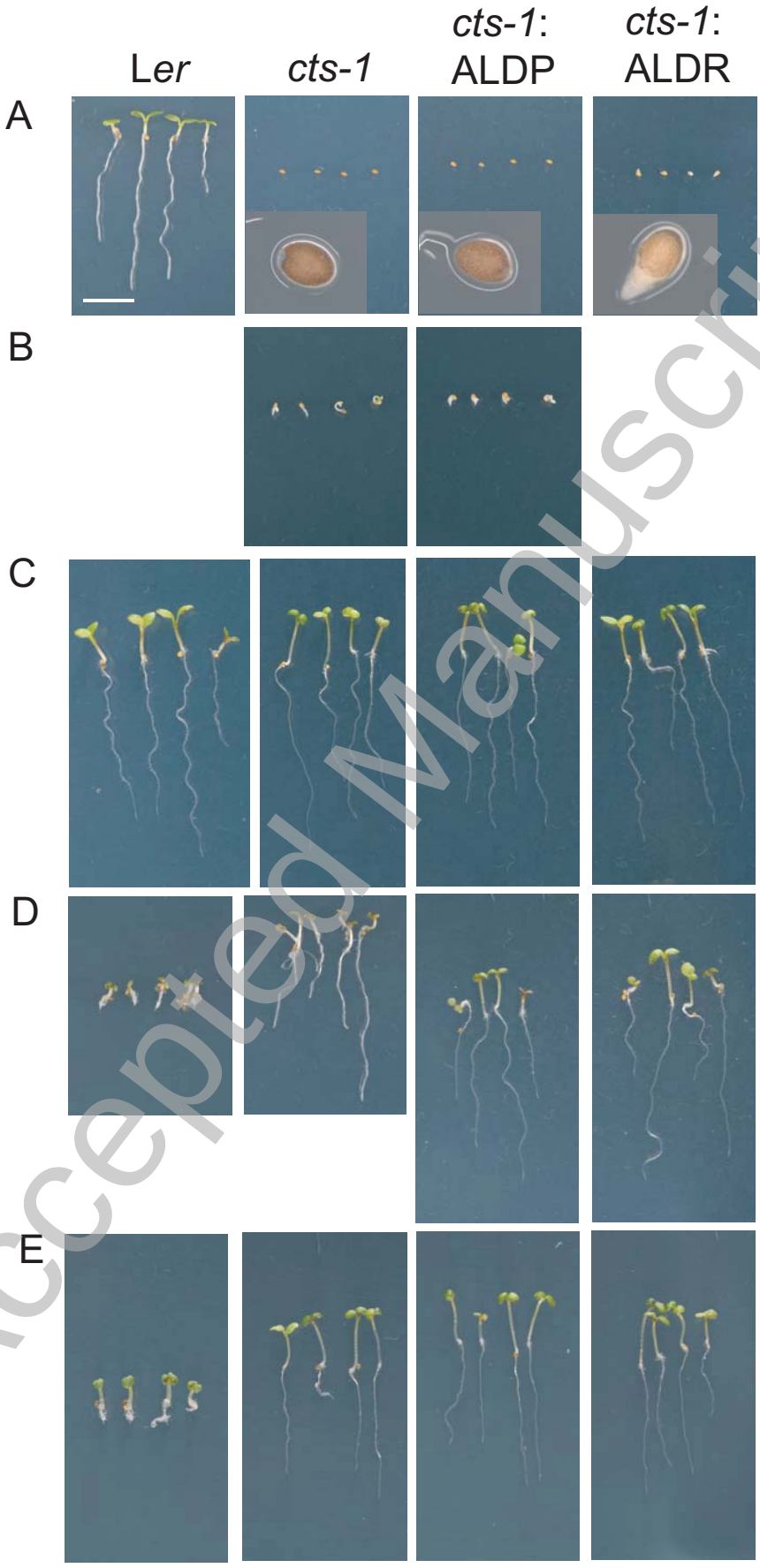

Fig. 7